An inverse method for the determination of full field stresses from experimentally measured normal strains

T-J Yu[1], **B V Sankar**[1]*, **N K Arakere**[1], and **R Vaidyanathan**[2]
[1]Department of Mechanical & Aerospace Engineering, University of Florida, Gainesville, Florida, USA
[2]Advanced Materials Processing and Analysis Center, Mechanical, Materials and Aerospace Engineering Department, University of Central Florida, Orlando, Florida, USA

The manuscript was received on 23 March 2006 and was accepted after revision for publication on 14 March 2007.

DOI: 10.1243/03093247JSA222

Abstract: Certain diffraction-based techniques that measure strains in bulk samples are limited to determination of normal strains. A numerical inverse method is developed to determine full field stresses from the experimentally determined normal strains in isotropic solids under plane stress conditions. The method is based on satisfying the equations of equilibrium and the constitutive relations. The finite difference method is employed to solve the equations and to determine the complete stress field. Furthermore, a least-squares procedure is used to determine the unknown functions of integration in conjunction with known values of shear stress along a reference line. The method is verified by using the normal strain fields in various specimens obtained using both finite element analysis and exact elasticity solutions. It is found that the proposed method predicts the shear stresses accurately in the examples considered.

Keywords: neutron diffraction, inverse problem, finite difference method, least square approximation

1 INTRODUCTION

Among the available experimental techniques for determining the internal strains in materials, diffraction-based techniques rely on using atomic planes as internal strain gauges. The distances between atomic planes, directly obtained from diffraction spectra, can be used to compute strains. The lattice strain $\varepsilon_{\phi\psi}$ along a general direction (ϕ, ψ) can be reported from the change in the interplanar spacing of crystal planes (h, k, l) oriented along (ϕ, ψ) as

$$\varepsilon_{\phi\psi} = \frac{d^{hkl}(\phi, \psi) - d_0^{hkl}}{d_0^{hkl}} \tag{1}$$

where d^{hkl} is the spacing of the plane subjected to stress and d_0^{hkl} is its spacing in the unloaded condition [**1**]. The origin of the stress can be either internal, i.e. residual, or external, i.e. applied in experiments that combine diffraction with mechanical loading. For the case of residual strain measurements, d_0^{hkl} is the spacing from a corresponding 'stress-free' specimen. While both neutrons and X-rays (from a conventional source) can be used for mechanical characterization, neutrons penetrate more deeply and are hence uniquely suited to studying the bulk behaviour of large polycrystalline samples. In a representative neutron diffraction experiment, equation (1) can be used to report normal strains along the scattering vector, defined as the difference between the wave vectors of the incident and scattered neutrons. This is shown in Fig. 1 for the case of a specimen subjected to a uniaxial compressive stress. Detector 1 records spectra that can be used to determine strains parallel to the loading direction while detector 2 records spectra that can be used to determine strains perpendicular to the loading direction. By measuring the strain in several orientations (at least six), in theory, it is possible to determine the complete strain tensor. However, in practice, difficulties arise in accurately orienting large samples and from errors associated with sample shifts

* *Corresponding author: Department of Mechanical & Aerospace Engineering, University of Florida, 231 MAE-A Building, PO Box 116250, Gainesville, Florida, 32611, USA. email: sankar@ufl.edu*

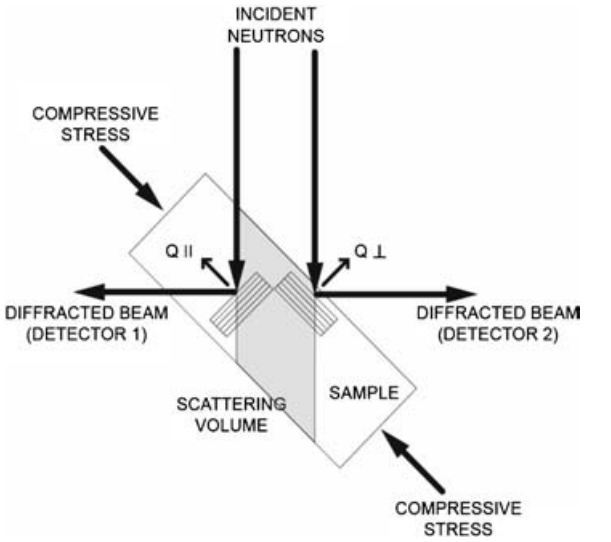

Fig. 1 Schematic diagram showing the direction of strains measured in a representative neutron diffraction experiment. ***Q*** is the scattering vector

and changes in the diffraction sampling volume. Hence, there is value in a general methodology that determines the complete stress and strain tensor from limited normal strain measurements such as those obtained from routine neutron diffraction experiments. Such a methodology is also applicable to comparable X-ray measurements from either conventional or synchrotron sources. This is of great importance in understanding material behaviour, e.g. the origin of cracks and load partitioning in composites, from experiments that combine external loading and diffraction. Furthermore, stresses often develop owing to a repair or joining process, e.g. welding. A quantitative assessment of these stresses is crucial in predicting the life of the component and also in predicting the integrity of the repair or joining process.

Hori and Kameda [**2**] proposed a method, called the stress inversion method, which is applicable only to a body in a state of plane stress or strain. It can estimate stress fields from displacements for materials whose constitutive relations are only partially known. While the method needs a strain distribution to compute three stress components, certain diffraction-based techniques can provide only the normal strains. A general computational procedure is presented for the determination of full strain and stress fields, knowing only the normal strains in an isotropic solid under plane stress conditions. Taking advantage of the equations of equilibrium and the constitutive relations, full field stresses can be computed from experimentally measured normal strains. When a numerical solution technique for inverse problems (mainly the finite difference (FD) method or the finite element (FE) method) is used to discretize the problem domain, a transformed system of algebraic equations containing unknown conditions is obtained. Yang and Chen [**3**] developed and Shaw [**4**] re-examined a linear least-squares method for solving the inverse problem. In this paper, a least-squares method is used to obtain the best estimation of unknown functions. With this new numerical method, diffraction techniques and other such methods that merely measure the normal strains could become more valuable.

2 OVERVIEW OF THE THEORY

The initial premise is that the experimentally determined normal strains in an isotropic elastic solid under plane stress conditions are known. The goal is to determine the complete stress and strain field in the elastic solid, by appropriately enforcing the compatibility conditions and stress equilibrium equations.

The known normal strain field in the computational domain is represented by the functions

$$\varepsilon_x = F(x, y) \tag{2}$$

$$\varepsilon_y = G(x, y) \tag{3}$$

By integrating the normal strains, the displacement field can be expressed as

$$u(x, y) = \hat{F}(x, y) + f(y) \tag{4}$$

$$v(x, y) = \tilde{G}(x, y) + g(x) \tag{5}$$

where $\hat{F}(x, y)$ is a function such that $\partial\hat{F}(x, y)/\partial x = F(x, y)$, $\tilde{G}(x, y)$ is a function such that $\partial\tilde{G}(x, y)/\partial y = G(x, y)$, and $f(y)$ and $g(x)$ are unknown functions.

The shear strain can be expressed as

$$\gamma_{xy} = \frac{\partial u}{\partial y} + \frac{\partial v}{\partial x} = \frac{\partial\hat{F}(x, y)}{\partial y} + f'(y) + \frac{\partial\tilde{G}(x, y)}{\partial x} + g'(x) \tag{6}$$

where a prime denotes ordinary differentiation with respect to the variable in the argument.

The normal and shear stresses can be expressed by invoking the constitutive relations and are given by

$$\sigma_x = C_{11}F(x, y) + C_{12}G(x, y) \tag{7}$$

$$\sigma_y = C_{12}F(x, y) + C_{22}G(x, y) \tag{8}$$

$$\tau_{xy} = \mu\gamma_{xy} = \mu\left[\frac{\partial\hat{F}(x, y)}{\partial y} + f'(y) + \frac{\partial\tilde{G}(x, y)}{\partial x} + g'(x)\right] \tag{9}$$

For the case of plane stress,

$$C_{11} = C_{22} = \frac{E}{1-\nu^2}, \quad C_{12} = \frac{\nu E}{1-\nu^2}, \quad \mu = \frac{E}{2(1+\nu)} \tag{10}$$

where E and ν are Young's modulus and Poisson's ratio respectively of the material. Substituting the stresses into the equilibrium equations [**5**] will result in the relations

$$\frac{\partial \sigma_x}{\partial x} + \frac{\partial \tau_{xy}}{\partial y} = C_{11}\frac{\partial F}{\partial x} + C_{12}\frac{\partial G}{\partial x} + \mu\left[\frac{\partial^2 \hat{F}(x,y)}{\partial y^2} + f''(y) + \frac{\partial G(x,y)}{\partial x}\right] = 0 \tag{11}$$

$$\frac{\partial \tau_{xy}}{\partial x} + \frac{\partial \sigma_y}{\partial y} = C_{12}\frac{\partial F}{\partial y} + C_{22}\frac{\partial G}{\partial y} + \mu\left[\frac{\partial F(x,y)}{\partial y} + \frac{\partial^2 \tilde{G}(x,y)}{\partial x^2} + g''(x)\right] = 0 \tag{12}$$

Note that it has been assumed that there are no body forces present. From the above equations, f'' and g'' can be determined as

$$f''(y) = -\frac{1}{\mu}\left(C_{11}\frac{\partial F}{\partial x} + C_{12}\frac{\partial G}{\partial x} + \mu\frac{\partial^2 \hat{F}}{\partial y^2} + \mu\frac{\partial G}{\partial x}\right) \tag{13}$$

$$g''(x) = -\frac{1}{\mu}\left(C_{12}\frac{\partial F}{\partial y} + C_{22}\frac{\partial G}{\partial y} + \mu\frac{\partial F}{\partial y} + \mu\frac{\partial^2 \tilde{G}}{\partial x^2}\right) \tag{14}$$

Integrating f'' and g'', $f'(y)$ and $g'(x)$ with two integration constants C_1 and C_2 are obtained as

$$f'(y) = -\frac{1}{\mu}\left(C_{11}\frac{\partial \tilde{F}}{\partial x} + C_{12}\frac{\partial \tilde{G}}{\partial x} + \mu\frac{\partial \hat{F}}{\partial y} + \mu\frac{\partial \tilde{G}}{\partial x}\right) + C_1 \tag{15}$$

$$g'(x) = -\frac{1}{\mu}\left(C_{12}\frac{\partial \hat{F}}{\partial y} + C_{22}\frac{\partial \hat{G}}{\partial y} + \mu\frac{\partial \hat{F}}{\partial y} + \mu\frac{\partial \tilde{G}}{\partial x}\right) + C_2 \tag{16}$$

Theoretically C_1 and C_2 must be constants over the entire field of measurement. However, in practice, it is found that there are slight variations depending on the accuracy of measurements as well as the numerical scheme described in the succeeding section. Hence the best values of the constants are sought using a least-squares error procedure. The variation in the value of the constants is presented by designating them as a function of x or y respectively. Equations (15) and (16) can be written as

$$f'(y) = -\frac{1}{\mu}\left(C_{11}\frac{\partial \tilde{F}}{\partial x} + C_{12}\frac{\partial \tilde{G}}{\partial x} + \mu\frac{\partial \hat{F}}{\partial y} + \mu\frac{\partial \tilde{G}}{\partial x}\right) + C_1(x) \tag{17}$$

$$g'(x) = -\frac{1}{\mu}\left(C_{12}\frac{\partial \hat{F}}{\partial y} + C_{22}\frac{\partial \hat{G}}{\partial y} + \mu\frac{\partial \hat{F}}{\partial y} + \mu\frac{\partial \tilde{G}}{\partial x}\right) + C_2(y) \tag{18}$$

where $C_1(x)$ and $C_2(y)$ are function of x and y respectively. Equation (17) can be written as

$$f'(y) = P(x,y) + C_1(x) \tag{19}$$

where f' is a function of y only. Consider equation (19) at a reference point $x = x_0$, which gives

$$f'(y) = P(x_0,y) + C_1(x_0) \tag{20}$$

Subtracting equation (20) from equation (19) gives

$$C_1(x) - C_1(x_0) = P(x_0,y) - P(x,y) \tag{21}$$

Define the left-hand side of equation (21) as

$$T(x) = C_1(x) - C_1(x_0) \tag{22}$$

Then equation (21) takes the form

$$T(x) = P(x_0,y) - P(x,y) \tag{23}$$

Theoretically T should be a function of x only. However, owing to inaccuracies in the measurement it will also vary slightly with y. The least-squares error approximation method is used to obtain the best estimate for $T(x)$ as

$$T(x) = \frac{1}{N_y}\sum_{i=1}^{N_y}[P(x_0,y_i) - P(x,y_i)] \tag{24}$$

where N_y is the number of point along the y axis at a certain x.

It should be noted that

$$T(x_0) \equiv 0 \tag{25}$$

Equation (24) can also be written for a specific $x = x_i$ as

$$T(x_i) = \frac{1}{N_y}\sum_{i=1}^{N_y}[P(x_0,y_i) - P(x_i,y_i)] \tag{26}$$

From equations (19) and (22), it is found that

$$f'(y) = P(x,y) + T(x) + C_1(x_0) \tag{27a}$$

A similar procedure is used to determine the function $g'(x)$ which then can be written as

$$g'(x) = Q(x, y) + S(y) + C_2(y_0) \tag{27b}$$

where the functions Q, S, and C_2 can be interpreted in the same way as for f' in deriving equation (27a). Note that the constants $C_1(x_0)$ and $C_2(y_0)$ cannot be uniquely determined. The value of shear stress at some point should be known in order to determine these constants.

3 NUMERICAL PROCEDURE

The analytical procedures described in the preceding section can be readily implemented in a numerical scheme. In order to perform the numerical differentiations used in the formulation, backward differences are employed. Backward differences are useful for approximating the derivatives if data in the future may depend on the derivatives approximated from the data in the past. In order to use backward differences in the present method, the initial value needs to be set equal to zero. A rectangular grid ($m \times n$) is generated in the domain where the normal strains are known at each point. The following steps are required to implement the numerical scheme.

Step 1. Create an $m \times n$ rectangular grid in the computational domain.

Step 2. Define $F(x, y)$ and $G(x, y)$ at each point from the normal strain data.

Step 3. Determine the values $\hat{F}$, $\tilde{F}$, $\hat{G}$, $\tilde{G}$, $\partial\hat{F}/\partial y$, $\partial\hat{G}/\partial y$, $\partial\tilde{F}/\partial x$, and $\partial\tilde{G}/\partial x$ at each point. By introducing the FDs Δx and Δy in space, these values are defined as

$$\hat{F}(i, j) = \begin{cases} 0 & \text{if } i = 0 \\ \sum_{i=1}^{m} \dfrac{F(i, j) + F(i-1, j)}{2} \Delta x \end{cases} \tag{28}$$

$$\hat{G}(i, j) = \begin{cases} 0 & \text{if } i = 0 \\ \sum_{i=1}^{m} \dfrac{G(i, j) + G(i-1, j)}{2} \Delta x \end{cases} \tag{29}$$

$$\tilde{F}(i, j) = \begin{cases} 0 & \text{if } j = 0 \\ \sum_{j=1}^{n} \dfrac{F(i, j) + F(i, j-1)}{2} \Delta y \end{cases} \tag{30}$$

$$\tilde{G}(i, j) = \begin{cases} 0 & \text{if } j = 0 \\ \sum_{j=1}^{n} \dfrac{G(i, j) + G(i, j-1)}{2} \Delta y \end{cases} \tag{31}$$

$$\frac{\partial}{\partial y}[\hat{F}(i, j)] = \begin{cases} 0 & \text{if } i = 0 \\ \dfrac{\hat{F}(i, j+1) - \hat{F}(i, j)}{\Delta y} \end{cases} \tag{32}$$

$$\frac{\partial}{\partial y}[\hat{G}(i, j)] = \begin{cases} 0 & \text{if } i = 0 \\ \dfrac{\hat{G}(i, j+1) - \hat{G}(i, j)}{\Delta y} \end{cases} \tag{33}$$

$$\frac{\partial}{\partial x}[\tilde{F}(i, j)] = \begin{cases} 0 & \text{if } j = 0 \\ \dfrac{\tilde{F}(i+1, j) - \tilde{F}(i, j)}{\Delta x} \end{cases} \tag{34}$$

$$\frac{\partial}{\partial x}[\tilde{G}(i, j)] = \begin{cases} 0 & \text{if } j = 0 \\ \dfrac{\tilde{G}(i+1, j) - \tilde{G}(i, j)}{\Delta x} \end{cases} \tag{35}$$

Step 4. Compute $f'(x, y)$ and $g'(x, y)$ at each point using equations (17) and (18).

Step 5. Then calculate the shear stress $\tau_{xy}(x, y)$ at each point using equation (9).

4 VERIFICATION OF THE METHOD

4.1 Comparison with FE method analysis

FE analysis was used to determine the normal strains in various data points in a specimen. These normal strains were used in the proposed method, and then the shear stresses were calculated. For verification of the method, these numerically calculated shear stresses were compared with the FE solutions. FE analysis was performed using four-node quadrilateral elements in ABAQUS™ and 1600 elements (40×40) and 1681 nodes were used in the model. The convergence of the method was studied by refining the FD grids from 10×10 to 40×40 in the present model.

A square aluminium plate of size 50.8 mm × 50.8 mm × 5.08 mm is clamped along an edge and a force of 2205 N is applied to one corner (Fig. 2). Young's modulus is taken as 70 GPa and Poisson's ratio as 0.33. Since the point load will cause a singular stress field in the vicinity of the point of application, the results were compared at locations away from the load. The shear stresses along the $y = 25.4$ mm line are plotted in Fig. 3. In order to determine the constants $C_1(x_0)$ and $C_2(y_0)$, the value of shear stress at some point should be known. In this example, the value of shear stress at the middle point of the $y = 25.4$ mm line was obtained from FE solution. The FE results are compared with the present inverse

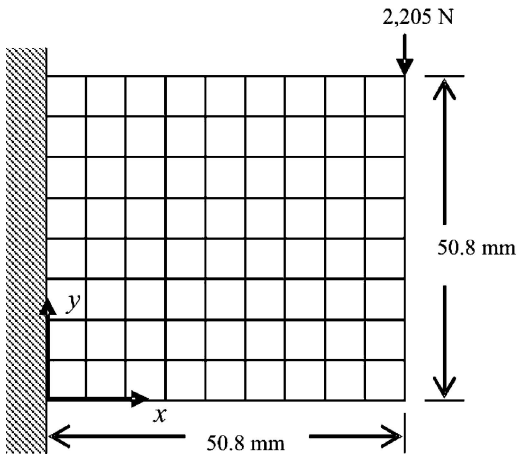

Fig. 2 Aluminium plate with uniform thickness

method for four different FD grid sizes. It may be noted that the present method compares well with the FE results except very close to the fixed support, and the 40×40 FD grid yields good results. The average error is 14 per cent and the maximum error is about 20 per cent (except for the point where the initial error occurs at the support). Table 1 displays the average error for different grid sizes (excluding the first two data points, which cause the initial error).

Table 1 Average error with different grid sizes

Grid size	Average error (%)
10×10	34.4
20×20	19.3
30×30	15.3
40×40	13.8

4.2 Comparison with analytical solutions

In the next example, a problem for which analytical solutions are available is solved. Thus the differences in the results are only due to that in the proposed method.

Consider the Brazilian disc specimen, which is a circular disc with a pair of diametrically opposite compressive loads as shown in Fig. 4. Hertz [**6**] developed the solution for the stresses in this specimen as

$$\sigma_x = -\frac{2P}{\pi B}\left[\frac{(R-y)x^2}{r_1^4} + \frac{(R+y)x^2}{r_2^4} - \frac{1}{D}\right]$$

$$\sigma_y = -\frac{2P}{\pi B}\left[\frac{(R-y)^3}{r_1^4} + \frac{(R+y)^3}{r_2^4} - \frac{1}{D}\right]$$

$$\tau_{xy} = \frac{2P}{\pi B}\left[\frac{(R-y)^2 x}{r_1^4} - \frac{(R+y)^2 x}{r_2^4}\right]$$

where $r_1^2 = (R-y)^2 = x^2$ and $r_2^2 = (R+y)^2 + x^2$

Step 1. Since the specimen is symmetric about the x and y axes, consider only one quarter of the specimen and make a grid $(m \times n)$ as shown in Fig. 5.

Step 2. Since the stress equations are provided, the normal strains can be defined as

$$F(x, y) = \varepsilon_x(x, y) = \frac{1}{E}\sigma_x(x, y) - \frac{\nu}{E}\sigma_y(x, y)$$

$$G(x, y) = \varepsilon_y(x, y) = \frac{1}{E}\sigma_y(x, y) - \frac{\nu}{E}\sigma_x(x, y)$$

Step 3. Perform the numerical calculation.

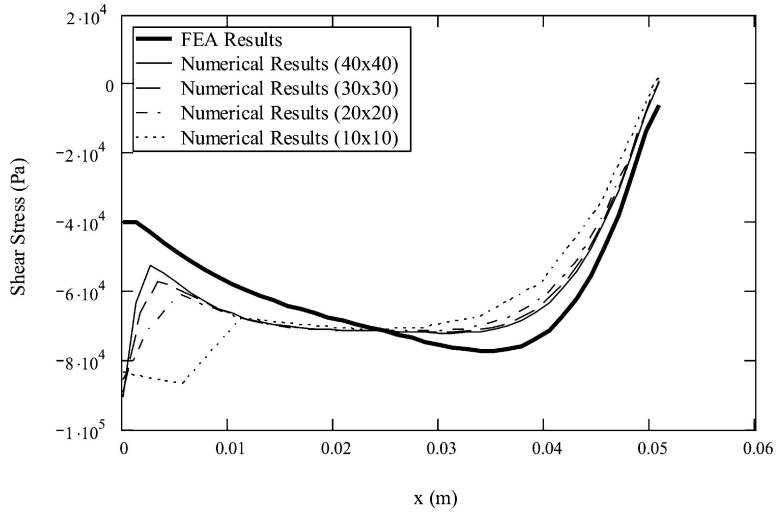

Fig. 3 Comparison of shear stresses for four FD grid sizes

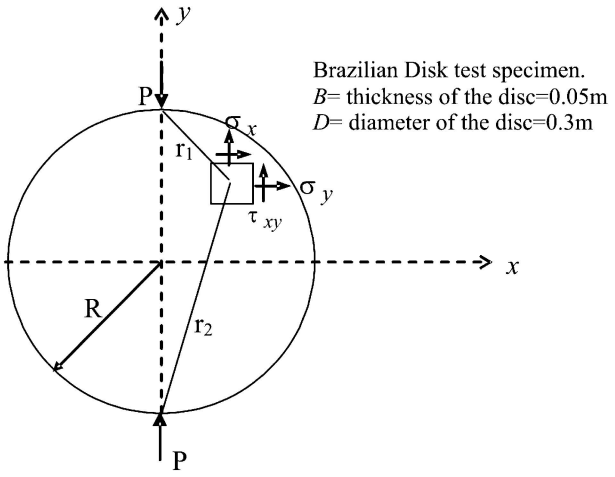

Fig. 4 Brazilian disc specimen

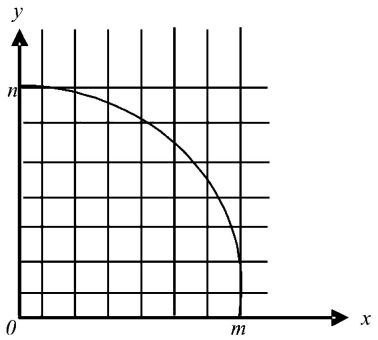

Fig. 5 A quarter of the specimen is taken as a domain

Then the shear stress can be computed by equation (9). Since the shear stress equation is given, the results from this method can be compared with the analytical solution. In the example a force of 300 MN is applied to the top (Fig. 4) and Young's modulus is taken as 200 GPa and Poisson's ratio as 0.3. The analytical shear stresses and the numerical shear stresses along the $y = 0.06$ m line are plotted in Fig 6. Since this specimen is symmetric about the y axis, it is expected that the shear stress is zero along the axis. This zero shear stress was used to determine the constants $C_1(x_0)$ and $C_2(y_0)$. The results shown in Fig. 6 were obtained using a 150×150 FD grid.

4.3 Comparison with analytical solutions in the local domain

In the previous example, an entire domain has been used for the numerical method. However, it is not always possible to obtain the normal strains in the entire domain of the specimen including boundaries. Typically methods such as the neutron diffraction method yield strains in a limited area of the specimen. In the next example, a local area is selected as the computational domain and the method verified. The same Brazilian disc specimen and the same boundary conditions are used for the method, except that the coordinates are translated to a new position (Fig. 7).

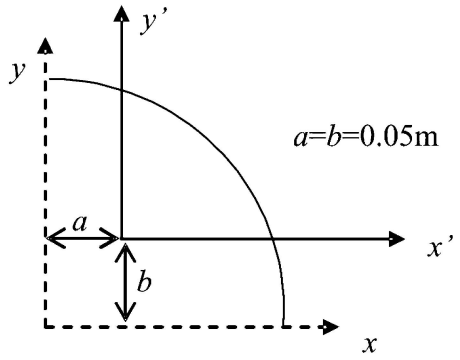

Fig. 7 Local area is taken from the entire domain by translating the coordinates

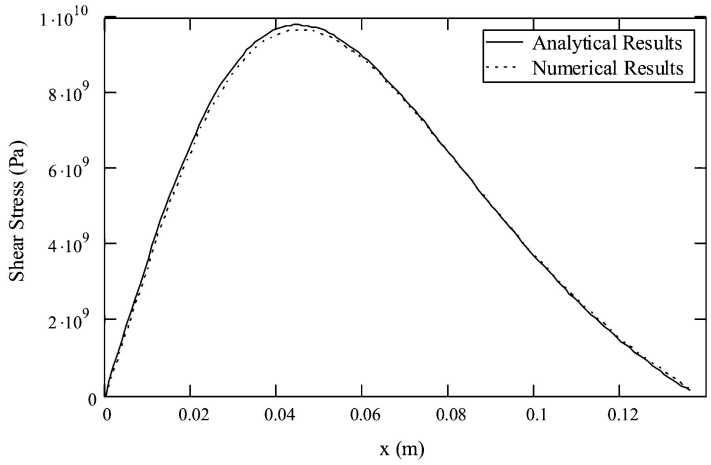

Fig. 6 Comparison of shear stresses obtained from the analytical solution and the present inverse method

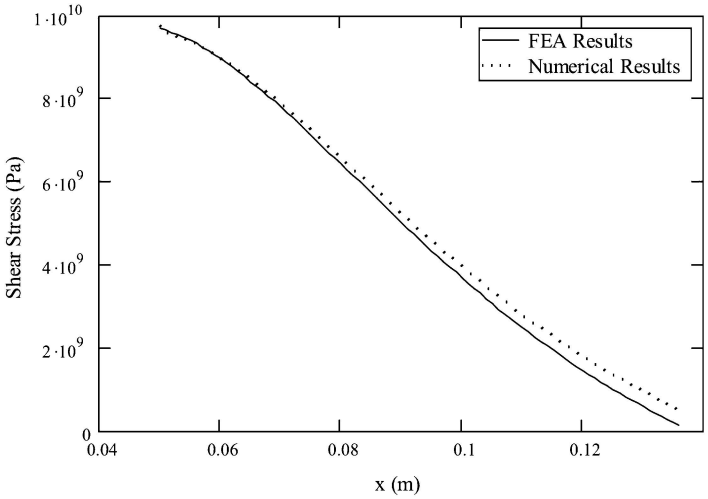

Fig. 8 Comparison of analytical and numerical solutions using a 100 × 100 FD grid (FEA, finite element analysis)

Since $x' = x + a$ and $y' = y + b$, the stress components can be rewritten as

$$\sigma_{x'} = -\frac{2P}{\pi B}\left\{\frac{[R-(y+b)](x+a)^2}{r_1^4} + \frac{[R+(y+b)](x+a)^2}{r_2^4} - \frac{1}{D}\right\}$$

$$\sigma_{y'} = -\frac{2P}{\pi B}\left\{\frac{[R-(y+b)]^3}{r_1^4} + \frac{[R+(y+b)]^3}{r_2^4} - \frac{1}{D}\right\}$$

$$\tau_{x'y'} = \frac{2P}{\pi B}\left\{\frac{[R(y+b)]^2(x+a)}{r_1^4} - \frac{[R+(x+b)]^2(x+a)}{r_2^4}\right\}$$

where $r_1^2 = [R-(y+b)]^2 + (x+a)^2$ and $r_2^2 = [R+(y+b)]^2 + (x+a)^2$.

Then using the aforementioned numerical procedures the shear stresses were calculated. The value of shear stress from analytical solution at the start point ($x = 0.05$ m, $y = 0.06$ m) was used to determine the constants. Figure 8 shows the analytical shear stresses and the numerical shear stresses along the same line ($y = 0.06$ m) as in the previous example.

5 DISCUSSION AND CONCLUSIONS

In the result of the first example (Fig. 3), a large amount of error was observed near the support, which is on the y axis. Setting the initial value on the y axis to be zero for the backward difference method may cause the initial error. In the second example (Fig. 6), however, zero is a good estimation for the initial value since the specimen is symmetric about the y axis. As shown in the results of the third example, it is observed that a finer mesh can minimize the initial error (Fig. 8).

A novel computational scheme has been developed in which the complete stress field can be determined from partial data for the normal strains. The method has been verified using two different methods. In the first method, FE analysis was used to generate information on normal strains, whereas the second method took advantage of available analytical elasticity solutions. After obtaining the normal strains, the proposed numerical method was implemented to calculate the shear stresses. The method yields accurate results for the shear stress field in several problems considered. The method will be a valuable tool in analysing normal strain measurements from diffraction-based methods and other such experimental techniques. Future work will include thermal residual stresses, orthotropic materials, and normal strains obtained from experimental measurements.

ACKNOWLEDGEMENTS

The authors are grateful for the support provided by the State of Florida Space Research Initiative to the University of Florida and the University of Central Florida.

REFERENCES

1 **Fitzpatrick, M. E.** and **Lodini, A.** (Eds) *Analysis of residual stress by diffraction using neutron and synchrotron radiation*, 2004 (Taylor & Francis, London).

2 **Hori, N.** and **Kameda, T.** Inversion of stress from strain without full knowledge of constitutive relations. *J. Mechanics Physics Solids*, 2001, **49**, 1621–1638.
3 **Yang, C. Y.** and **Chen, C. K.** The boundary estimation in two-dimensional inverse heat conduction problems. *J. Phys. D: Appl. Phys.*, 1996, **29**, 333–339.
4 **Shaw, J.** Noniterative solution of inverse problems by linear least square method. *Appl. Math. Modeling*, 2001, **25**, 683–696.
5 **Timoshenko, S. P.** and **Goodier, J. N.** *Theory of elasticity*, 3rd edition, 1971 (McGraw-Hill, New York).
6 **Hertz, H.** *Gesammelte Werke* (*Collected works*), 1895 (J. A. Barth, Leipzig).